ANL/MSD/CP - 95854
CONF-980764--

RADIATION DAMAGE FROM SINGLE HEAVY ION IMPACTS ON METAL SURFACES*

S. E. Donnelly[1] and R. C. Birtcher[2]

[1]Joule Physics Laboratory
University of Salford
Manchester M5 4WT
United Kingdom

[2]Materials Science Division
Argonne National Laboratory
9700 S. Cass Ave.
Argonne, IL 60439

June 1998

Submitted to the International Society for Optical Engineering, Laser and Materials in Industry, July 13-16, 1998, Quebec City, Canada.

*Work supported by the U. S. Department of Energy, Office of Basic Energy Sciences, under Contract W-31-109-Eng-38 at Argonne National Laboratory and by a collaborative research grant number 910670 from NATO.

DISCLAIMER

DISCLAIMER

Portions of this document may be illegible in electronic image products. Images are produced from the best available original document.

Radiation damage from single heavy ion impacts on metal surfaces

Stephen E. Donnelly[a] and Robert C. Birtcher[b]

[a]Joule Physics Laboratory, Science Research Institute,
University of Salford, Manchester M5 4WT, UK

[b]Materials Science Division, Argonne National Laboratory, Argonne, IL 60439

ABSTRACT

The effects of single ion impacts on the surfaces of films of Au, Ag, In and Pb have been studied using *in-situ* transmission electron microscopy. On all these materials, individual ion impacts produce surface craters, in some cases, with associated expelled material. The cratering efficiency scales with the density of the irradiated metal. For very thin Au foils (≈20–50nm), in some cases individual ions are seen to punch small holes completely through the foil. Continued irradiation results in a thickening of the foil. The process giving rise to crater and hole formation and other changes observed in the thin foils has been found to be due to pulsed localised flow — i.e. melting and flow due to the thermal spikes arising from individual ion impacts. Experiments carried out on thin films of silver sandwiched between SiO_2 layers have indicated that pulsed localised flow also occurs in this system and contributes to the formation of Ag nanoclusters in SiO_2—a system of interest for its non-linear optical properties. Calculation indicates that, when ion-induced, collision cascades occur near surfaces (within ≈ 5nm) with energy densities sufficient to cause melting, craters are formed. Crater formation occurs as a result of the explosive outflow of material from the hot molten core of the cascade. Processes occurring in the sandwiched layer are less well understood.

Keywords: particle/solid interactions, ion irradiation, transmission electron microscopy (TEM), craters, thermal spikes.

1. INTRODUCTION

The idea of so-called 'spikes' resulting from individual ion impacts was first discussed in the scientific literature in the 1950s by Brinkman[1]. Although, the interaction of an energetic ion with a solid can be described successfully, below a certain energy density, as a series of binary collisions involving the impinging ion and recoiling substrate atoms in what is normally described as a collision cascade, Brinkman pointed out that this description is inadequate when the mean free path between displacement collisions approaches the interatomic spacing of the substrate. Under these circumstances, a highly disturbed region is formed, in which the mean kinetic energy of the atoms may be up to several eV; this is known as an energy or displacement spike. A short time after the initial energy deposition the kinetic energy in the spike may be shared in a relatively continuous distribution by all the atoms within the spike region and this may give rise to an effective temperature within the spike zone significantly above that required for melting—this phase is generally referred to as a thermal spike. Spikes are small—typically of the order of a few nanometres in diameter and techniques with a high spatial resolution must be used to obtain information about their structure. In addition, they are of short duration (≈ 10ps) so that measurements on processes resulting from ion impacts usually take place a relatively long time after the impact. Any measurement is thus of the effects of the displacement spike, the ensuing thermal spike and any defect annealing processes that may subsequently take place.

In the last decade or so the availability of high powered computers has enabled molecular dynamics (MD) simulations to be carried out on assemblies of atoms sufficiently large to handle spike effects, although, as yet, primary recoil energies are limited to about 20 keV. These studies have shown that, at times a few picoseconds or so after the simulated impact of a heavy ion incident on a crystalline metal, a spike zone may be formed in which an analysis of atom positions and energies reveals a radial pair distribution function typical of a fluid (or an amorphous solid) and an effective temperature significantly above melting[2,3]. In addition, some experimental work has provided evidence that spike effects may be responsible for amorphous zones in some crystalline semiconductor materials[4,5] and disordered zones in ordered metallic alloys.[6]

Additional author information:
SED—Email s.e.donnelly@physics.salford.ac.uk —Web: http://www.salford.ac.uk/physics/staff/s.e.donnelly/
RCB—Email birtcher@anl.gov

In this paper we review our recent work[7-9] on the effects of individual spikes on metal surfaces using transmission electron microscopy of specimens that are undergoing ion irradiation *in-situ* in the TEM. Although the bulk of the work has been carried out on thin gold specimens, studies on thin films of Ag, In, Pb and SiO_2/Ag/SiO_2 sandwich structures are also presented.[10]

2. EXPERIMENTAL

Ion irradiations were carried out in a Hitachi A-9000 transmission electron microscope (TEM) operating at 300 keV at the IVEM/Accelerator Facility located at Argonne National Laboratory. Thin Au films were made by thermal evaporation of 99.999 at. % pure starting material onto NaCl at a temperature of 350°C. This resulted in a largely monocrystalline film with a <100> surface normal. Thinner specimens, used for the observations of single-ion induced holes were prepared by jet-polishing[11] 99.999 at. % pure Au with grain size greater than 10 μm having a (110) texture. Grains used for observations were those with <110> surface normal. Specimens of Ag, Pb and In were produced from rolled, annealed foils with a 99.999 at.% purity from which 3 mm discs were punched and electrochemically thinned. The gold films were determined by Rutherford backscattering to have a thickness of 62 ± 2 nm; the thickness of the electropolished Au specimens was not precisely known but measurement using electron energy loss spectrometry indicated that no holes were formed in regions thicker than 50 nm. The thickness of the other electrochemically polished specimens was not accurately known but was of the order of 100 nm. SiO_2/Ag/SiO_2 sandwiches were grown by electron-beam deposition of a 15-nm thick Ag layer on bulk SiO_2 followed by deposition (also with an electron beam) of 150 nm of SiO_2 in a vacuum of 10^{-7} Torr. TEM specimens were prepared by core-drilling a 3 mm diameter disk, grinding the centre of the disk from the bulk SiO_2 side to near perforation, then finally ion milling to perforation. The ion milling completely removed the SiO_2 surface layer in the area directly adjacent to the perforation; however TEM observations were performed only in areas where all three layers remained intact. In the IVEM/Accelerator Facility, the ion beam is oriented 30° from the microscope axis; in our experiments the specimen was tilted 15° towards the ion beam so that both ions and electrons were incident on the specimen at 15° to the foil normal. Specimens were irradiated with various ions at energies in the range 50 – 800 keV at dose rates between 10^{10} and 10^{12} ions/cm²/s.

Craters on the metal films were made visible in TEM in the same way as voids and bubbles by means of their phase-contrast under controlled amounts of objective lens defocusing. Images were generally obtained in bright field, on a region of the (somewhat bent films) in which no Bragg reflection was strongly excited. Under these conditions, underfocusing the objective lens by typically 1000 nm yields reasonably sharp images in which the crater is lighter than the background and is delineated by a dark Fresnel fringe. Similarly a small mound or particle on the surface appears darker than the background with a light fringe around it. A similar degree of *over*focus gives rise to images in which this contrast is reversed, i.e. small craters appear darker than the background and small particles appear lighter than the background.

In addition to normal photographic recording, images from a Gatan 622 video camera and image-intensification system were viewed with total magnifications of approximately 2 million, and recorded on video tape with a time resolution of 33 ms.

3. CRATER FORMATION ON THIN FILMS

Figure 1a, b and c show images of craters created by single ions of Kr, Au and Xe incident on a 62 nm gold film at 200 keV. Fig. 1d shows a somewhat larger crater resulting from an impact of a 600 keV Au ion. These images have been digitised from videotape recordings of the experiments and show craters that are similar to those reported by Merkle and Jäger[12] for Au

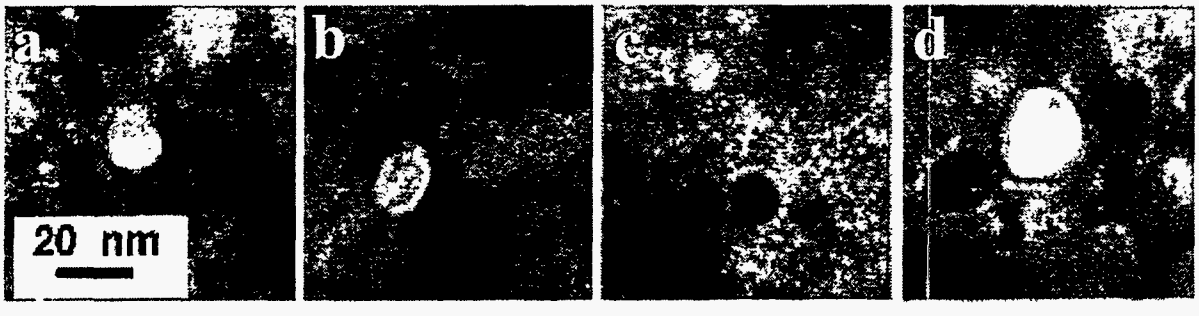

Fig. 1. Underfocused TEM images of craters resulting from impacts of Au with individual heavy ions: a) 200 keV Xe^+, b) 200 keV Kr^+, c) 200 keV Au^+, d) 600 keV Au^+.

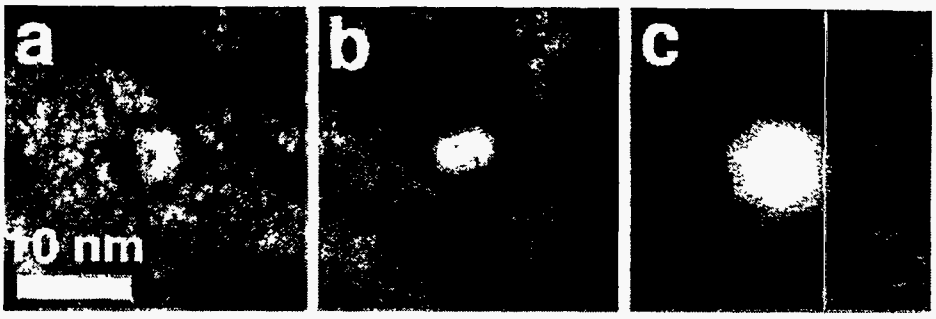

Fig. 2. Ion impact craters: a) 100 keV Xe^+ on In, b) 200 keV Xe^+ on Ag and c) 200 keV Xe^+ on Pb.

irradiated with Bi^+ and Bi_2^+ ions following *ex-situ* irradiations. Note that the incomplete Fresnel fringe on one side of the crater in Fig. 1a indicates that the crater bottom is tilted and intersects the surface. Note also that the features exhibiting reverse underfocus contrast to that of the craters, i.e. dark with a light Fresnel fringe, are particles on the surface. Frame-by-frame analysis of video recordings of the experiments indicate that both these and the craters appear between video frames. At the dose rates used in the experiments, 2.4 x 10^{11} ions/cm^2/s, on average one ion passes through the area of each image in Fig.1 every two video frames—implying that features occurring between individual frames result from single impacts (an observation confirmed by experiments at lower dose rates). Stereo microscopy has been carried out on a number of specimens in order to determine whether craters form on the irradiated surface or the back surface of the films. Essentially, at energies where there is little or no probability of a cascade intersecting the rear surface of the film (e.g. $\leq$ 50 keV) craters form only on the irradiated surface. As the energy is increased, however, there is an increasing probability of crater formation on the rear surface of the foils also. There is no discernible difference in appearance between the craters on the front and back surfaces and in images digitised from videotape it is not possible to distinguish between them. At the dose rates used in our experiments, craters are generally annihilated in a few seconds by subsequent impacts. This will be discussed further in section 4.

Although, the bulk of our work on ion-induced cratering has been concerned with gold, we have also carried out a systematic study of other materials which has revealed that the phenomenon is by no means confined to gold[9]. Figure 2 shows images of craters due to impacts of Xe ions on Pb, Ag and In. These images have, once again, been digitised from video recordings made without interruption of the continuous irradiation. Fig. 2a shows a rare, small crater found on an indium film subjected to 400 keV Xe irradiation at a temperature of 17 K. Experiments were initially carried out on indium at room temperature and these failed to reveal any cratering; however, it was thought possible that the high homologous temperature (0.69 T_m) for this material at room temperature may have resulted in a very rapid thermal annealing of craters by surface and bulk diffusion processes — although craters were being created, they may not have survived sufficiently long to be recorded on videotape. To test this possibility, indium specimens were irradiated with 400 keV Xe^+ ions at 17 K using a cryogenic specimen holder in the TEM. A frame-by-frame analysis of the video recording of this experiment revealed the very occasional formation of craters at this temperature. Specifically, two craters were observed during $\approx$30 minutes of ion irradiation implying a creation efficiency (very approximately) of 5 x 10^{-5} craters/ion.

Figure 2b shows a small crater on Ag irradiated with 100 keV Xe ions. In general, craters in this material were observed to be qualitatively similar to those on gold although the creation efficiency (6 x 10^{-3}) was almost an order of magnitude lower. As with gold, large irregular craters up to 10 nm in diameter were occasionally observed and all craters were observed to be filled in discretely as a result of subsequent ion impacts. Studies of heavy-ion irradiation of a thin Ag layer sandwiched between two layers of SiO_2 were also carried out and will be briefly discussed in section 7.

Finally, Fig. 2c shows a faceted crater on Pb resulting from the impact of a 200 keV Xe^+ ion at room temperature. In general, images of craters in this material, were less clear than in the case of gold, due to the higher degree of defocus that had to be used to image the craters. (The defocus used was typically 9 μm underfocus c.f. 1 μm for Au. The necessity for a higher degree of defocus probably indicates that the craters were shallower in this case than for Au). Unlike gold, there was little evidence of material ejected from the craters visible as particles on the surface. Crater creation efficiency for Pb was 7 x 10^{-3}. As with gold and silver, the observed craters are thermally stable at room temperature when the ion irradiation is halted but under conditions of continual irradiation are annihilated discretely by subsequent ion impacts.

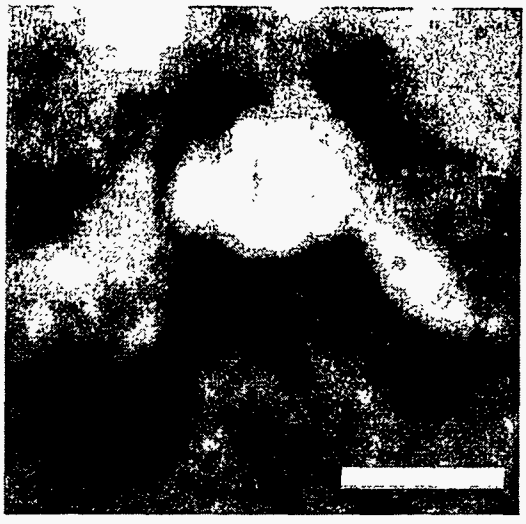

Fig 3. Large crater on Au due to the impact of a 400 keV Xe ion. Scale marker indicates 10 nm.

A detailed analysis of the cratering efficiency under heavy-ion irradiation has been published elsewhere[9] and has enabled us to define the criteria required for spike-induced cratering to occur:

(i) the atoms within the core of the spike must receive sufficient energy for the region to melt (albeit for a very small period of time),

and

(ii) the spike must be located within a short distance from a surface (estimated to be of the order of 5 nm). For heavy ions in the energy range 50–800 keV.

Criterion (i) necessitates that the density of the metal be above a value of approximately 7 g/cm^3 for cratering to occur.

Although many of the impact craters on all materials tend to be small without direct signs of expelled material, we believe that the most instructive examples are those larger craters in which expelled material is also clearly observed. Fig. 3 shows a particularly interesting example. The contrast in this figure is consistent with a crater and an accompanying quenched droplet of molten material that has been ejected on ion impact. (The light contrast to the right of this crater is the remnant of a pre-existing crater). If it is assumed that the expelled material in this case has cylindrical symmetry, then it contains approximately 20,000 gold atoms. If all the material in this droplet came from the adjacent crater, the crater would be approximately 4 nm deep.

4. CRATER ANNIHILATION

The static images discussed so far give an incomplete picture of the crater formation process. For example, the 'live' image recorded on videotape during continuous irradiation of Au films with 200 keV Xe ions, reveals a rapidly changing crater population with approximately 7 craters in the field of view (110 nm x 85 nm) at any time. At the dose rate used in the experiment, statistically, there is one ion impact per second through the area of Fig. 4. The efficiency of crater creation on gold is of the order of 6% (ranging from 2% to 10%) implying that the majority of ion impacts annihilate craters without creating new ones. Typically, craters survive a few seconds at a dose rate of 2.4 x 10^{11} ions/cm^2/s.

An example of the 'life cycle' of a crater on Au at room temperature, under continuous irradiation is illustrated in Fig. 4 by a series of 3 images numbered according to their video frame. As an ion passes through the area shown, on average, every 30 frames, a discrete change occurring between video frames is clearly the result of a single ion impact. Discontinuous changes occurred between frames 2 and 3 and between frames 51 and 52. The figure shows a crater ≈7.5 nm in diameter formed as a

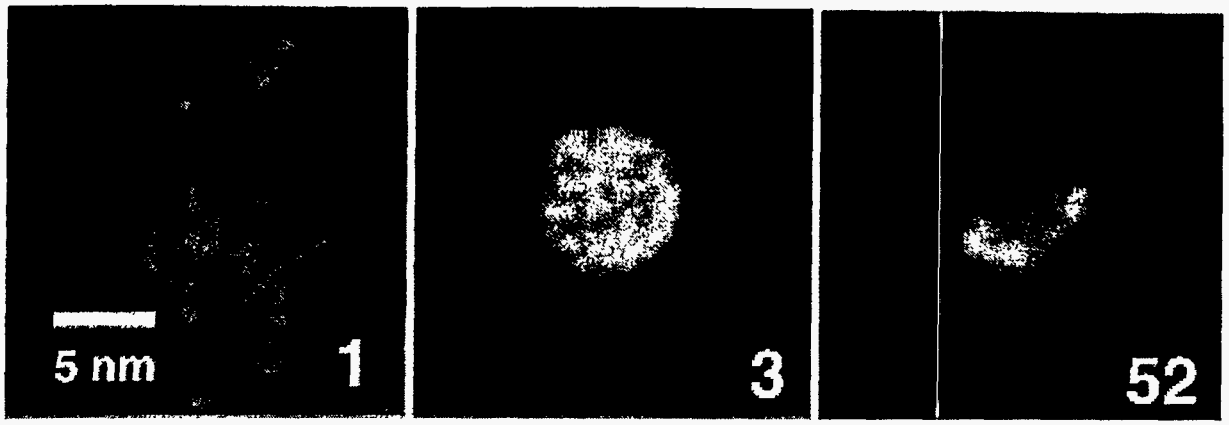

Fig. 4. Creation and annihilation of a crater on Au as a result of impacts of 400 keV Xe^+ ions. The numbers are video frame numbers and thus represent time in units of 1/30 s. Discrete changes occurred immediately prior to frame 3 (creation) and frame 52 (partial annihilation).

result of a single 400 keV Xe ion impact. The crater then remains essentially unchanged for just over 50 video frames (≈1.7 seconds) after which time a discrete event causes flow of material into the crater resulting in its partial obliteration. A few seconds later (not shown), the remaining contrast disappears in a second discrete event. Note that, in this particular case, no new crater was observed to form within the field of view (approximately 6 times the area shown) at the moment that the crater was filled in. However, in other cases, material expelled during the creation of a crater is seen to fill-in a second nearby crater.

Crater lifetimes on gold, at room temperature under irradiation with Xe ions have been studied at three energies, 50 keV, 200 keV and 400 keV.[8] When the ion beam is turned off, craters are thermally stable for measured periods of several weeks; however, under steady-state conditions of continual irradiation, at a dose rate of 2.4×10^{11} ions/cm^2/s, craters have a lifetime in the range 1–12 s at all three ion energies studied. Small craters are generally annihilated in a single discrete event whereas larger craters disappear in two or more steps. Lifetime measurements on 14 craters with a mean diameter of 4.4 nm yield a mean lifetime of 4.9 s for craters annihilated in a single step. With the assumption that all ion impacts are capable of annihilating existing craters, the Xe ion has an annihilation cross section for small craters of approximately 85 nm^2, i.e. an ion impact within a radius of approximately 5 nm of the centre of a small crater will annihilate the crater. The precise mechanism of crater annihilation, however, has not been elucidated. Although, flow processes have been directly observed when material from a new crater annihilates an existing one, in the majority of cases, spikes must occur within the film and not at the surface and do not give rise to craters. Nonetheless, it does appear that such events result in crater annihilation, occurring as discrete events. This would seem to indicate that either (i) interstitials expelled from the spike arrive at the surface where they may annihilate a crater or (ii) the effects at the surface of a thermal spike located below the surface are sufficient to thermally anneal craters. At present we have no experimental means of distinguishing between these two possibilities.

5. HOLE FORMATION IN THIN FILMS

In addition to experiments on vacuum evaporated films we also carried out experiments on thin electrochemically thinned gold foils.[7] Although we also observe crater formation, our most striking observation was that in the thinnest areas of the foil many single ion impacts resulted in the creation of holes having diameters between 5 and 10 nm as shown in Fig. 5. In the figure a previously formed hole (A) is somewhat modified, in the region indicated by the arrow, when a second hole (B) is formed in close proximity. Note that contrast visible in the hole is due to noise in the imaging system. Once again the dose rate is such that the hole results from a single ion impact.

Approximately 1% of the Xe ions produced holes. Electron energy loss measurements in the area shown in Fig. 5, made with a 50 nm diameter electron beam, indicate that no holes were created in regions with thickness greater than about 50 nm. However, the wedge-shaped nature of the foil in the area of the holes makes it probable that the area, at the edge of the foil, where the holes are formed was thinner than this, perhaps on the order of 20 nm. This thickness is consistent with Monte-Carlo calculations, using TRIM-95,[13] of the ability of 200 keV Xe ions to produce damage though the entire depth of an Au foil.

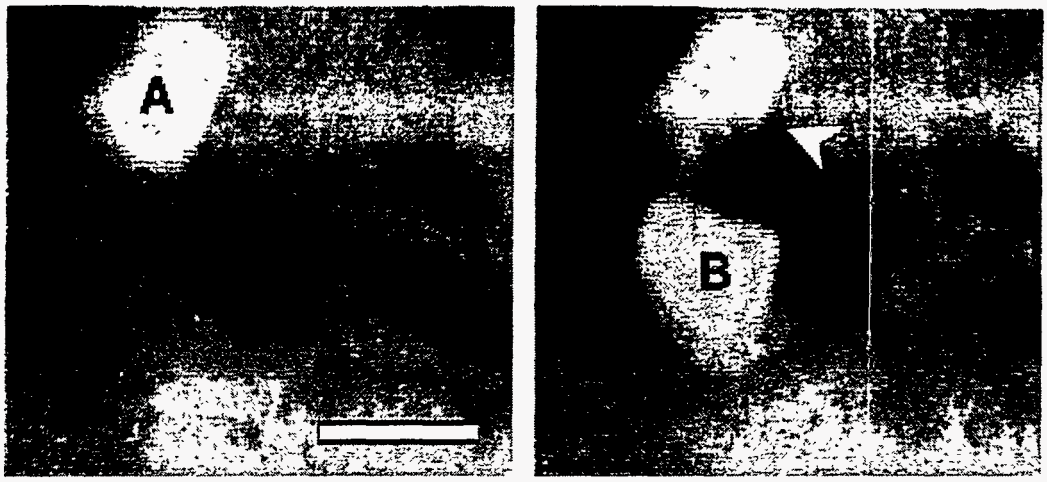

Fig. 5. Formation of a hole in a thin gold foil due to the impact of a single 200 keV Xe^+ ion. Images are from successive video frames. Scale marker represents 10 nm.

Of the order of 1 ion in 200 generates a displacement cascade that extends to both surfaces of a 50 nm thick Au layer suggesting that the displacement cascade must extend through the entire specimen thickness in order to produce a hole.

An ion strikes the area shown in Fig. 5 on average every 10 frames (≈0.3 s). The holes in the figure appear between successive video frames (within a time period of 1/30th second). Assuming a foil thickness between 20 to 50 nm, between 20,000 to 50,000 gold atoms were removed to create hole (B). This would imply a very large sputtering yield if the atoms were ejected from the gold surface. However, the change in image contrast suggest that these atoms have been moved to the specimen surface. As with craters, holes appear to be formed as a consequence of flow processes associated with thermal spikes. Note that craters are also observed on one or the other surface in these thin foil specimens.

As with the craters, many ion impact events change the shape of existing holes. Changes in hole shape appear to be due to cascade events that do not produce new holes but generate plastic flow near to existing ones as, for instance can be seen in the change that occurs to hole (A) in Fig. 5. Although an energetic ion impact may initially give rise to an explosive outflow of material, during the quenching phase of the molten zone to the solid state, surface tension forces will act on any free surfaces included in the melt zone. This gives rise to changes in the shape of edges and the tendency of holes to become more circular. At the extreme limit of changes in hole shape, small holes are also observed to be occasionally filled in by cascade events that do not themselves leave a hole or crater.

6. FILM THICKENING — PULSED LOCALISED FLOW

It has been a frequent observation in our laboratories that thin areas of Au specimens disappear as a consequence of thickening during heavy-ion irradiation. The dynamics of this process are illustrated in Fig. 6 which shows a thin area surrounding a hole. An ion strikes the area shown on average every four video frames. When observed at a high dose-rate the film morphology is observed to change in a manner similar to changes that occur when thin gold foils are heated to close to the bulk melting temperature and surface tension forces act on the material. A frame-by-frame analysis, however, reveals that changes are again discrete and are due to individual ion impacts. Specifically, between frames 1 and 3 of the figure, the foil morphology changes due to an ion impact probably in the region indicated by the letter 'A'. The structure remains relatively constant until an impact in region 'B' just before frame 140 causes another significant modification. A similar discrete events occurs just prior to frame 216 in the region marked with the letter 'C'. The tendency in each discrete event is for the film to thicken under the influence of localised melting and surface tension forces. As in the case of hole production, only a small fraction of ion impacts result in major changes. We describe this process as pulsed localised flow and illustrate it schematically in Fig. 7. An electrochemically, jet-polished film has a thickness that generally tapers towards a central hole or holes—a thin area used for electron microscopy thus has a wedge shaped cross-section which is modified, as illustrated schematically in Fig. 7 by each successive ion impact.

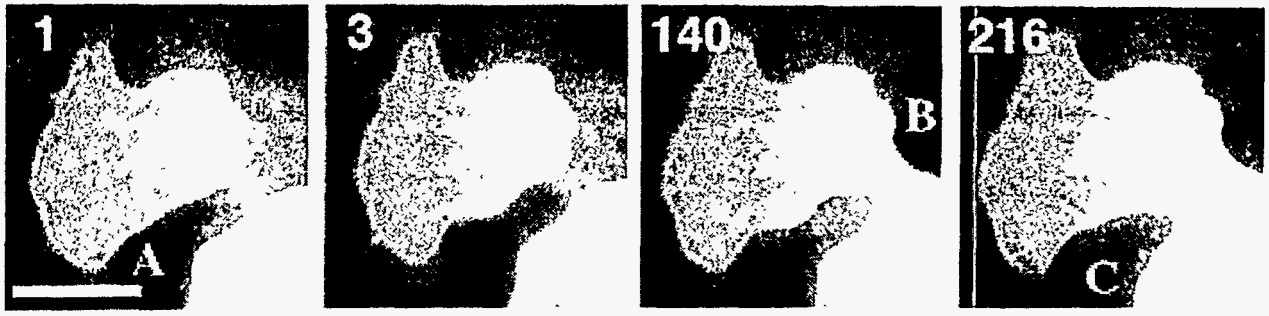

Fig. 6. Changes to a gold foil as a result of 200 keV Xe^+ irradiation at room temperature. The numbers indicate the video frame from which the image was taken, recorded at 30 frames per second. The scale marker indicates 20 nm.

We believe that events such as those recorded in Fig. 6 are the first observations of such an ion-induced, pulsed, localised flow process. MD simulations by Averback *et al.* of a 20 keV Au ion incident on Au[3] lend support to the existence of such a plastic flow process. They found a cascade region of the order of 6 nm in diameter by 6 nm in depth in which atoms had a mean energy of approximately 2 eV. At 7.0 ps after ion impact, a crater remained which they described as resulting from viscous flow of the melt zone to the surface.

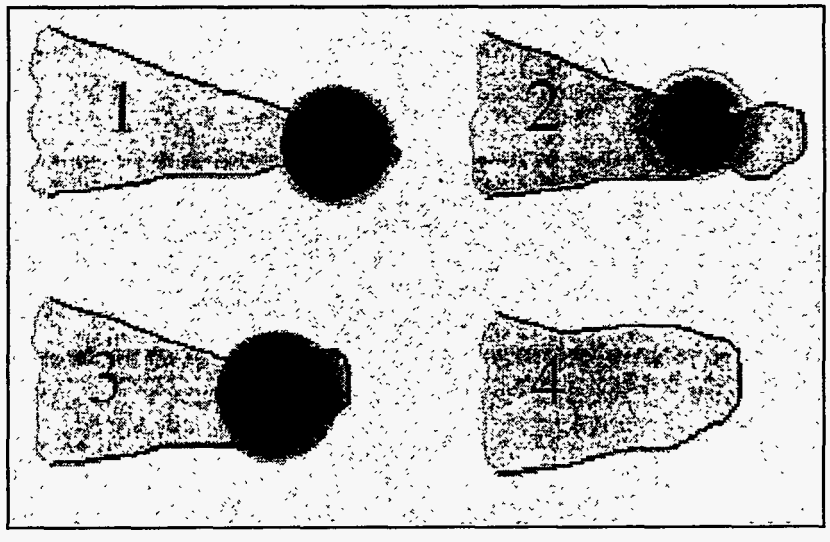

Fig. 7. Schematic illustration of pulsed localised flow in a foil with a wedge-shaped cross section.

7. ION IMPACT EFFECTS IN AN INSULATOR/METAL SANDWICH

All of the observations reported so far are of ion impact effects on free surfaces of metal films. Ion impact effects are also of interest in a system in which the metal film does not have free surfaces—metal-SiO_2 multilayers—as ion beam processing of such systems has been found to give rise to embedded metallic nanoclusters in a dielectric matrix. Such systems exhibit non-linear optical properties with many potential optoelectronic applications. Although several methods have been used to synthesize these systems, including high-temperature glass fusion, sputtering, sol-gel ion exchange, and ion implantation, it has been recently demonstrated[14] that ion-beam mixing of metal-SiO_2 multilayers can also be used to create metallic clusters in an SiO_2

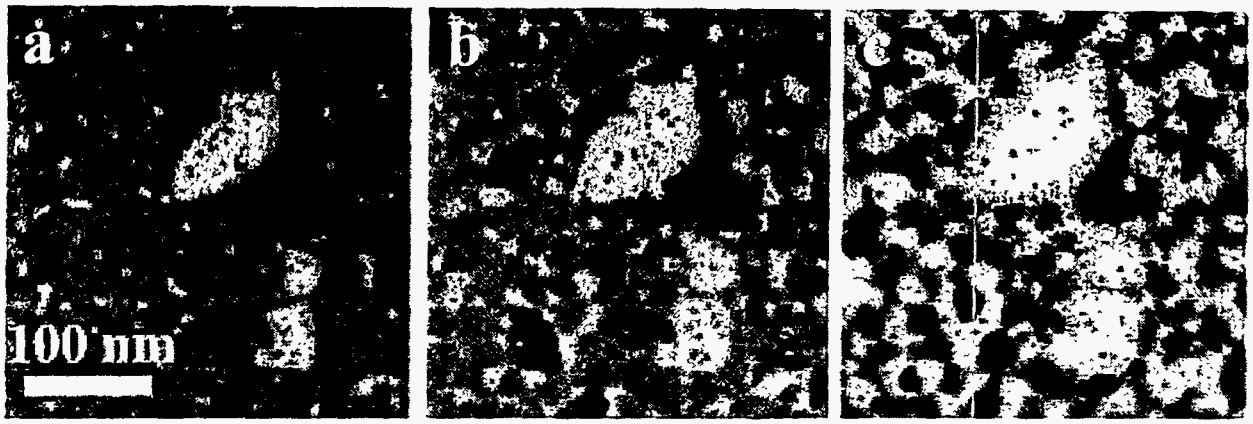

Fig. 8. Changes taking place in a SiO_2/Ag/SiO_2 sandwich as a result of irradiation with 400 keV Xe^+ ions. a) unirradiated, b) irradiated to a dose of 3 x 10^{15} ions/cm^2, c) irradiated to a dose of 6 x 10^{15} ions/cm^2. The lighter areas in the images are holes in the Ag layer—the SiO_2 layers are intact in these areas.

substrate over depths of only a few micrometers. In an attempt to elucidate the mechanisms responsible for the transformation of the metal-SiO_2 multilayer into the embedded nanocluster system, we have carried out *in-situ* experiments on a simple sandwich structure consisting of a 15 nm Ag film between two SiO_2 layers, one of which is 150 nm thick; the other being thinned to an unknown thickness for TEM observations.[10] Ion irradiation induced two distinct processes in this system:

(i) Conversion of the thin, two-dimensional Ag film into three-dimensional microcrystals (diameter >30nm), and

(ii) Formation of Ag nanoclusters (diameter <10nm) which can be observed in regions uncovered by the retreating Ag film.

Both processes can be seen clearly in Fig. 8, which displays a series of TEM images of the same area of the SiO_2/Ag/SiO_2 sample during irradiation to progressively higher doses with 400 keV Xe ions. All holes visible after the highest ion dose are traceable to initial holes or grain boundaries. The process appears to involve the conversion of individual crystalline grains in the film from a 2-dimensional to a 3-dimensional structure. As the holes increase in size, Ag that has been dispersed by the Xe beam into the SiO_2 observed to form the nanoclusters.

Neither the precise mechanism whereby a film sandwiched between two SiO_2 layers is able to flow nor that responsible for nanocluster formation is yet fully understood. However, explanation of the former process appears to lie in the same pulsed localised flow responsible for morphological changes in free standing films as discussed in section 6. Further work is underway on this system in our laboratories.

8. CONCLUSIONS

Spike effects produce surface cratering in materials in which cascades can be produced near to surfaces and with energy densities sufficient to cause melting. In particular, for heavy ion irradiation of materials whose density is greater than approximately 7 g/cm^3, craters may occur where the spikes resulting from individual impacts occur with centres within ≈ 5nm of the surface. Crater formation occurs as a result of the explosive outflow of material from the hot molten core of the spike. In foils where the spikes extend entirely through the thickness, holes form as a result of individual ion impacts. Both craters and small holes may be annihilated by the transport of material—by flow or diffusion—from the site of subsequent impacts or by annealing due to the thermal spike resulting from subsequent impacts. In addition, pulsed localised flow—in which spike-induced melting and flow occur under surface tension forces—has been identified as a major cause of morphological change in dense metal films. Finally, pulsed localised flow also appears to operate on metal films embedded in a metal-insulator sandwich structure and may be an essential component of the mechanism of ion-beam induced nanocluster formation.

ACKNOWLEDGEMENTS

We should like to thank B. Kestel for specimen preparation, and E. Ryan, L. Funk, T. McCormick, P.M. Baldo and S. Ockers for assistance with the *in-situ* TEM experiments. This work has been supported by the U.S. Department of Energy, BES-Materials Sciences, under Contract W-31-109-Eng-38 and by a collaborative research grant number 910670 from NATO. One of us (SED) acknowledges funding from the Materials Science Division at Argonne National Laboratory which has enabled him to make extended visits to ANL.

REFERENCES

1. J. A. Brinkman, J. Appl. Phys. **25**, 951, 1954.
2. T. Diaz de la Rubia, R. S. Averback , H. Hsieh, R. Benedek, J. Mater. Res. **4** (3), 579, 1989.
3. R. S. Averback, J. Nuc. Mat **216,** 49, 1994.
4. M. O. Ruault, J. Chaumont , J. M. Penisson and A. Bourret , Phil. Mag. **A 50**, 667, 1984.
5. J. Narayan, O.S. Oen, D. Fathy and O.W. Holland, Materials Letters **3**, 67, 1985.
6. M. L. Jenkins, and M.Wilkens, Phil. Mag. **34,** 1155, 1976.
7. R. C. Birtcher and S. E. Donnelly, Phys. Rev. Letters **77** (21), 4374, 1996.
8. S. E. Donnelly and R. C. Birtcher, Phys. Rev. **B 56** (21), 13599, 1997.
9. S. E. Donnelly and R. C. Birtcher, Phil. Mag. A, to be published, 1998.
10. S. E. Donnelly, R. C. Birtcher, L. Thomé and L. Rehn. Work in preparation.
11. B. J. Kestel, Ultramicroscopy **25**, 351, 1988.
12. K. L. Merkle and W. Jager, Phil. Mag. **A 44**, 741, 1981.
13. J. F. Ziegler, J. P. Biersack and U. Littmark, *The Stopping and Ranges of Ions in Solids,* (Pergamon Press, NY), 1985.
14. F. Garrido, J.C. Dran, L. Thomé, C. Meneghini, F. Gonella and A. Quaranta, Nucl. Instrum. Meth. **B 115**, 561, 1996.